Actin cap associated focal adhesions and their distinct role in cellular mechanosensing

Dong-Hwee Kim[1,2], Shyam B. Khatau[1,2], Yunfeng Feng[1,3], Sam Walcott[1,4], Sean X. Sun[1,2,4], Gregory D. Longmore[1,3*] & Denis Wirtz[1,2*]

[1] Johns Hopkins Physical Sciences in Oncology Center, The Johns Hopkins University, Baltimore, Maryland 21218, USA

[2] Department of Chemical and Biomolecular Engineering, The Johns Hopkins University, Baltimore, Maryland 21218, USA

[3] Departments of Medicine and Cell Biology and Physiology, Washington University School of Medicine, St. Louis, MO 63110, USA

[4] Department of Mechanical Engineering, The Johns Hopkins University, Baltimore, Maryland 21218, USA

[*] To whom correspondence should be addressed. Email: wirtz@jhu.edu or glongmor@dom.wustl.edu

This document contains the following supplementary information:

Supplementary figures S1 to S10

Legends to supplementary figures S1 to S10

Legends to supplementary movie 1 to 3

Figure S1

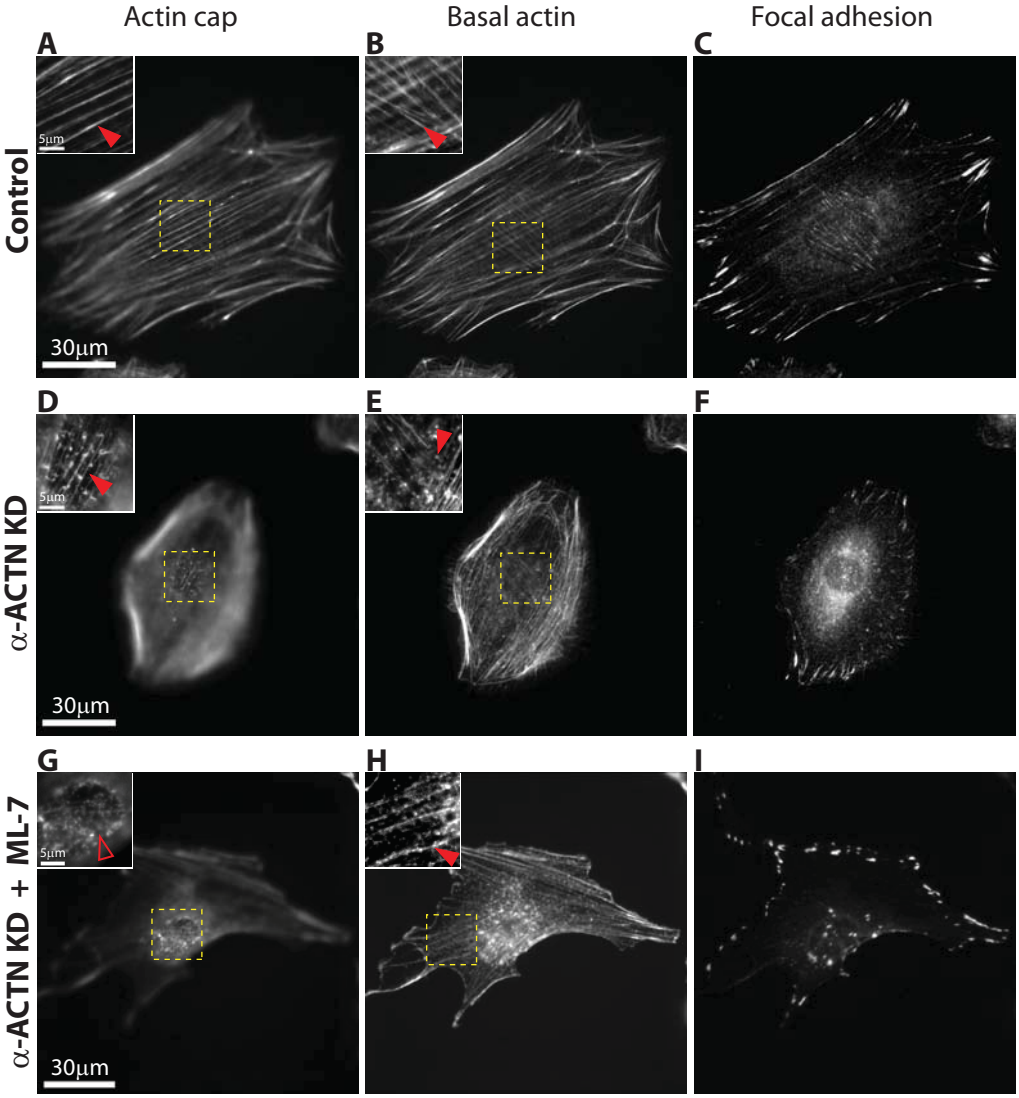
Actin cap
Basal actin
Focal adhesion
A
B
C
Control
5μm
30μm
D
E
F
α-ACTN KD
5μm
30μm
G
H
I
α-ACTN KD + ML-7
5μm
30μm

Figure S2

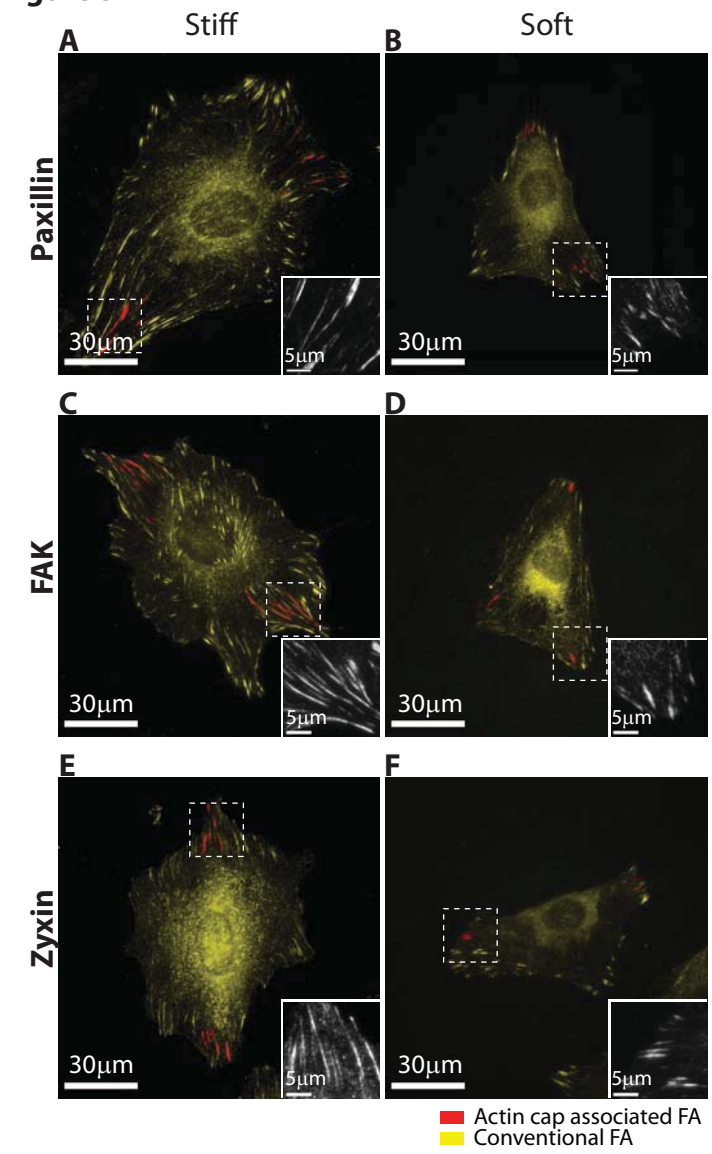
A
Stiff
B
Soft
Paxillin
C
D
FAK
E
F
Zyxin
30μm
5μm
Actin cap associated FA
Conventional FA

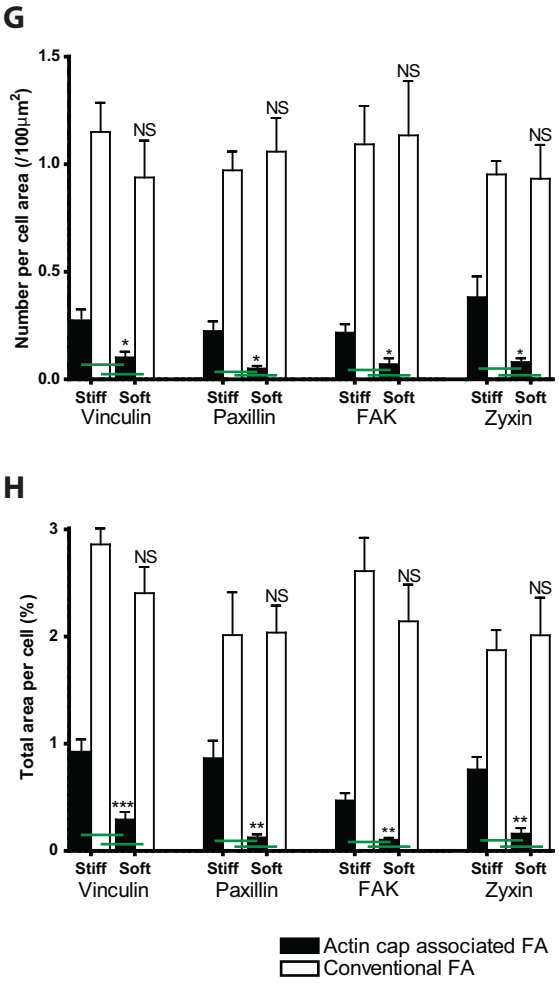
G
Number per cell area (/100μm²)
NS
*
Stiff Soft
Vinculin
Paxillin
FAK
Zyxin
H
Total area per cell (%)
***
**
Actin cap associated FA
Conventional FA

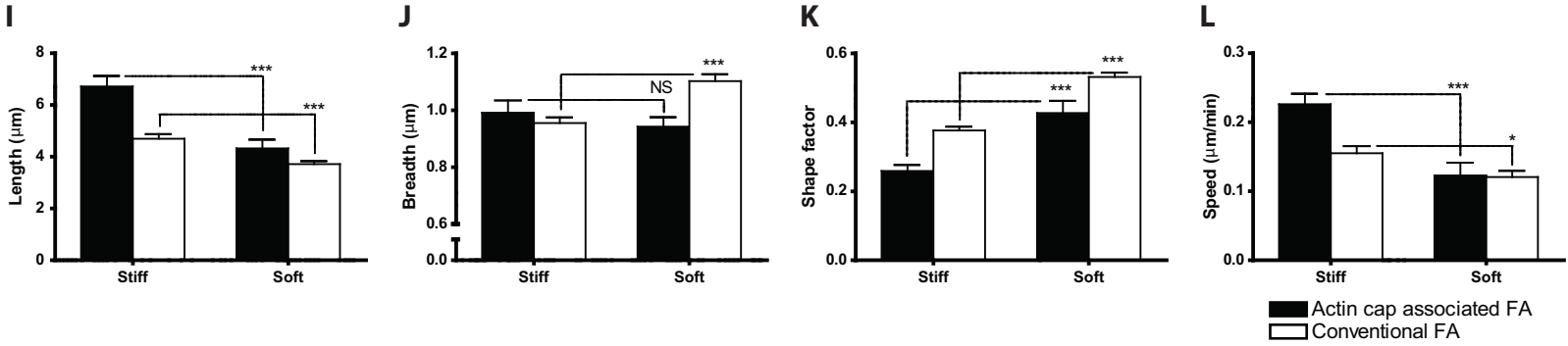
I
Length (μm)
J
Breadth (μm)
K
Shape factor
L
Speed (μm/min)
***
NS
*
Stiff
Soft
Actin cap associated FA
Conventional FA

Figure S3

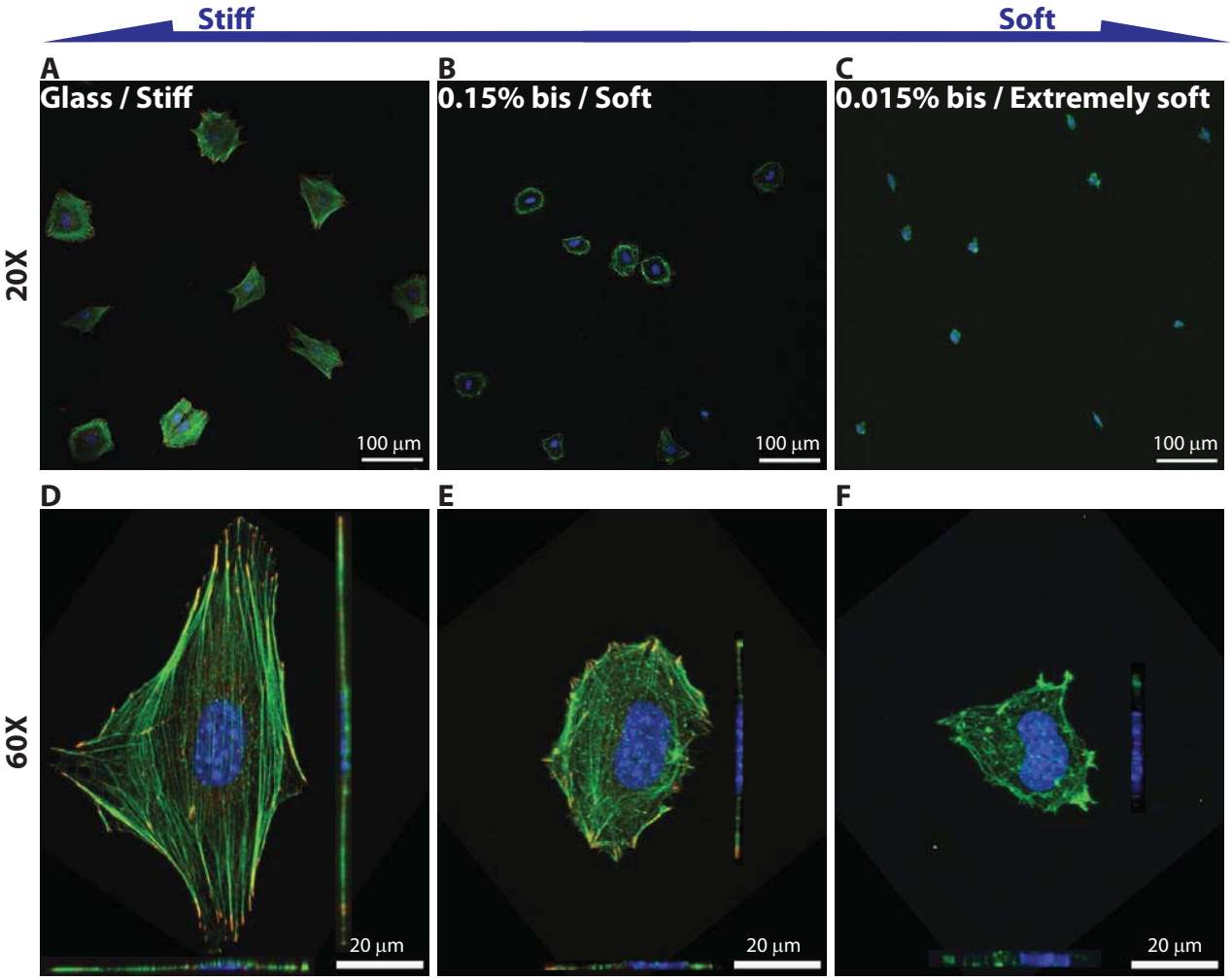
Stiff
Soft
A
Glass / Stiff
B
0.15% bis / Soft
C
0.015% bis / Extremely soft
20X
100 µm
100 µm
100 µm
D
E
F
60X
20 µm
20 µm
20 µm

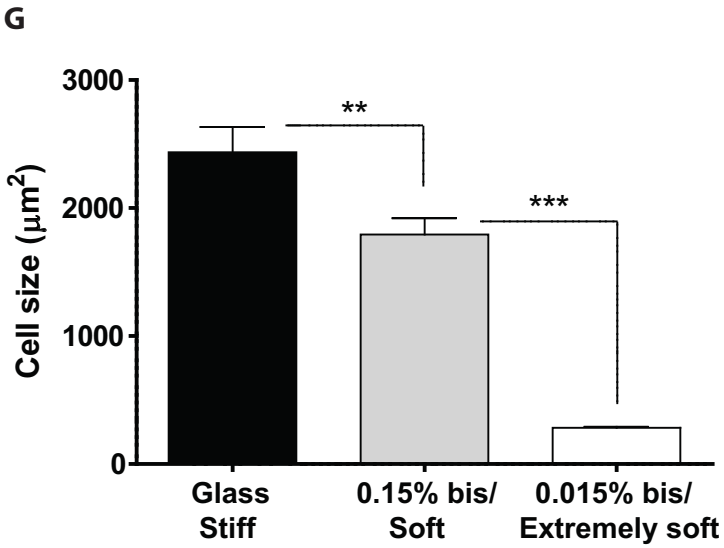
G
3000
2000
1000
0
Cell size (µm²)
**
***
Glass
Stiff
0.15% bis/
Soft
0.015% bis/
Extremely soft

Figure S4

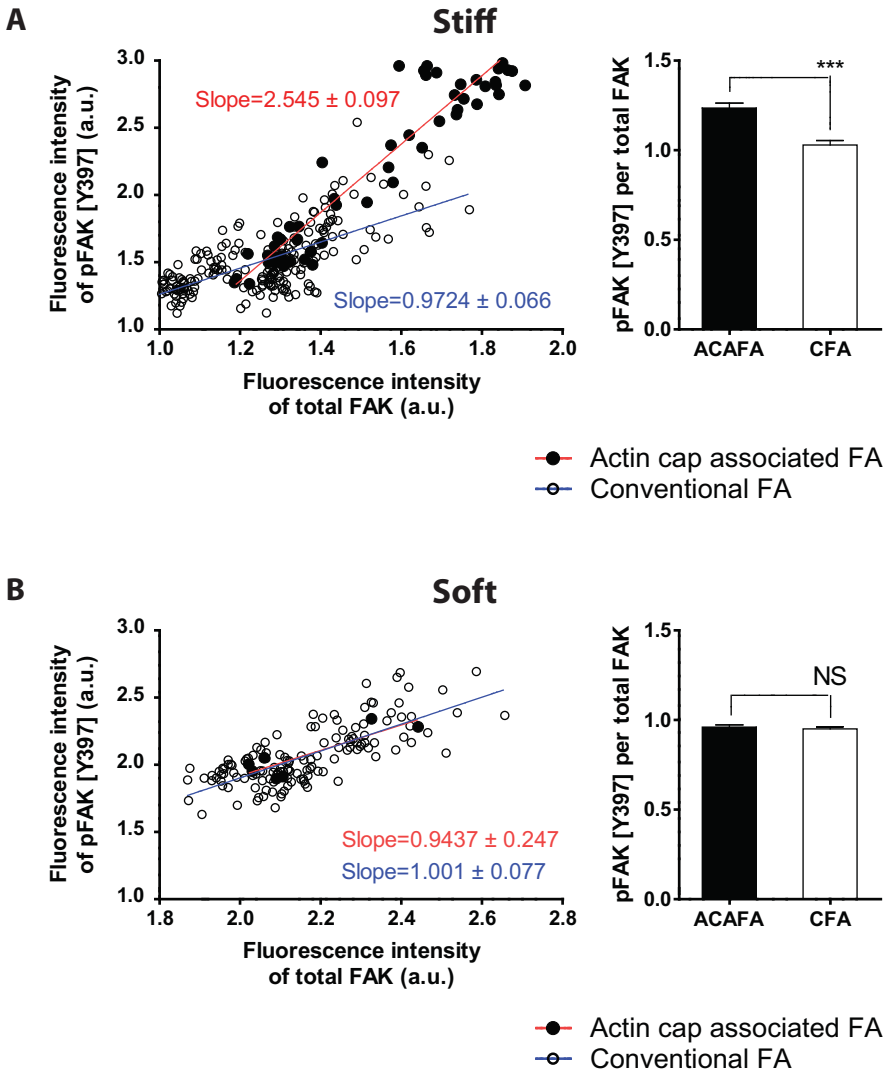
A
Stiff
Slope=2.545 ± 0.097
Slope=0.9724 ± 0.066
Fluorescence intensity of pFAK [Y397] (a.u.)
Fluorescence intensity of total FAK (a.u.)
pFAK [Y397] per total FAK
***
ACAFA
CFA
Actin cap associated FA
Conventional FA
B
Soft
Slope=0.9437 ± 0.247
Slope=1.001 ± 0.077
Fluorescence intensity of pFAK [Y397] (a.u.)
Fluorescence intensity of total FAK (a.u.)
pFAK [Y397] per total FAK
NS
ACAFA
CFA
Actin cap associated FA
Conventional FA

Figure S5

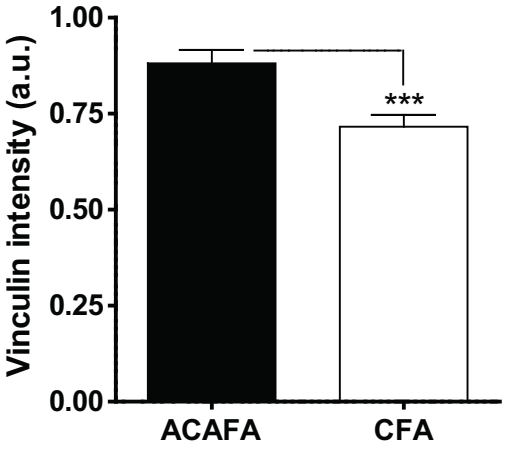

Figure S6

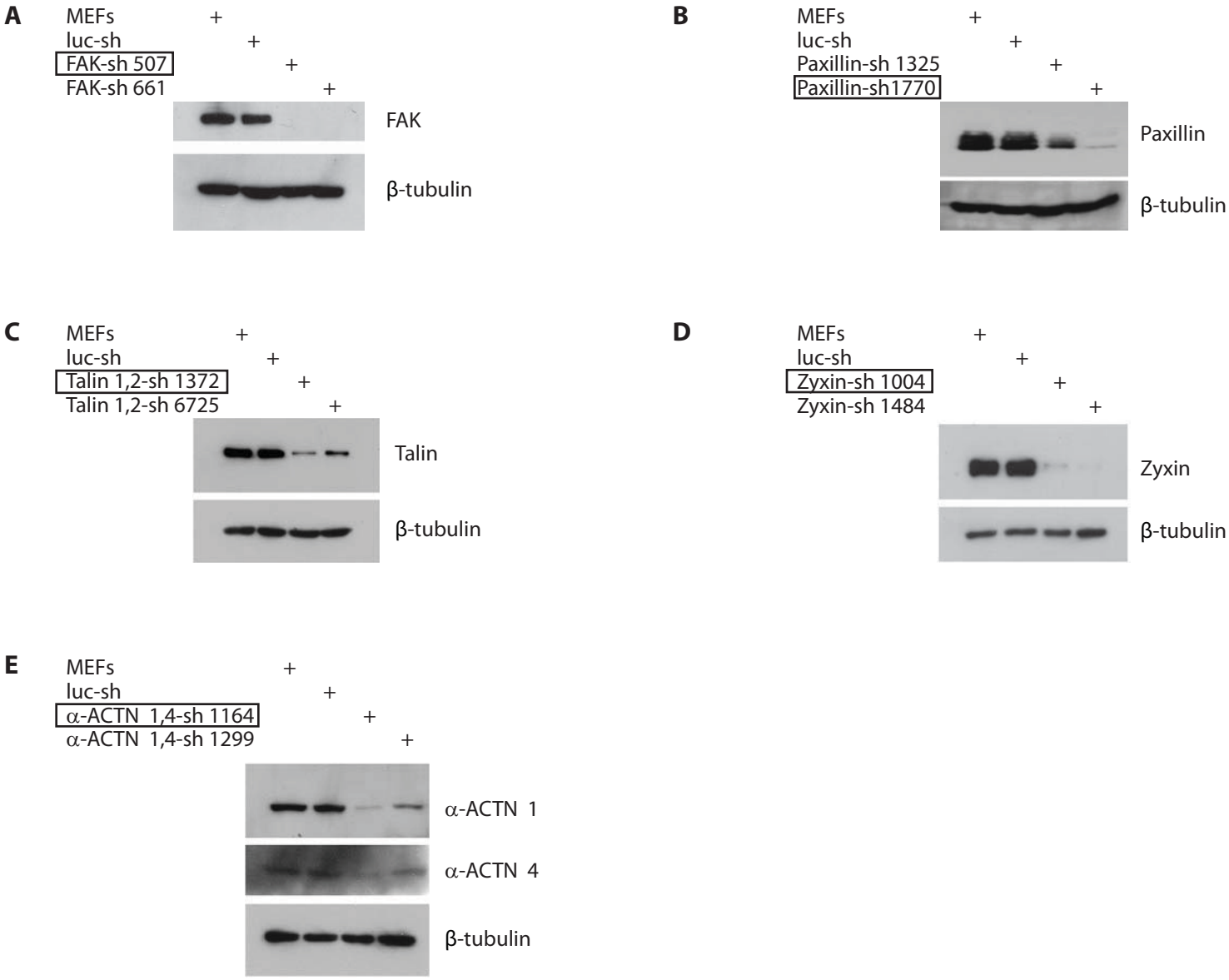
A
MEFs +
luc-sh +
FAK-sh 507 +
FAK-sh 661 +
FAK
β-tubulin
B
MEFs +
luc-sh +
Paxillin-sh 1325 +
Paxillin-sh1770 +
Paxillin
β-tubulin
C
MEFs +
luc-sh +
Talin 1,2-sh 1372 +
Talin 1,2-sh 6725 +
Talin
β-tubulin
D
MEFs +
luc-sh +
Zyxin-sh 1004 +
Zyxin-sh 1484 +
Zyxin
β-tubulin
E
MEFs +
luc-sh +
α-ACTN 1,4-sh 1164 +
α-ACTN 1,4-sh 1299 +
α-ACTN 1
α-ACTN 4
β-tubulin

Figure S7

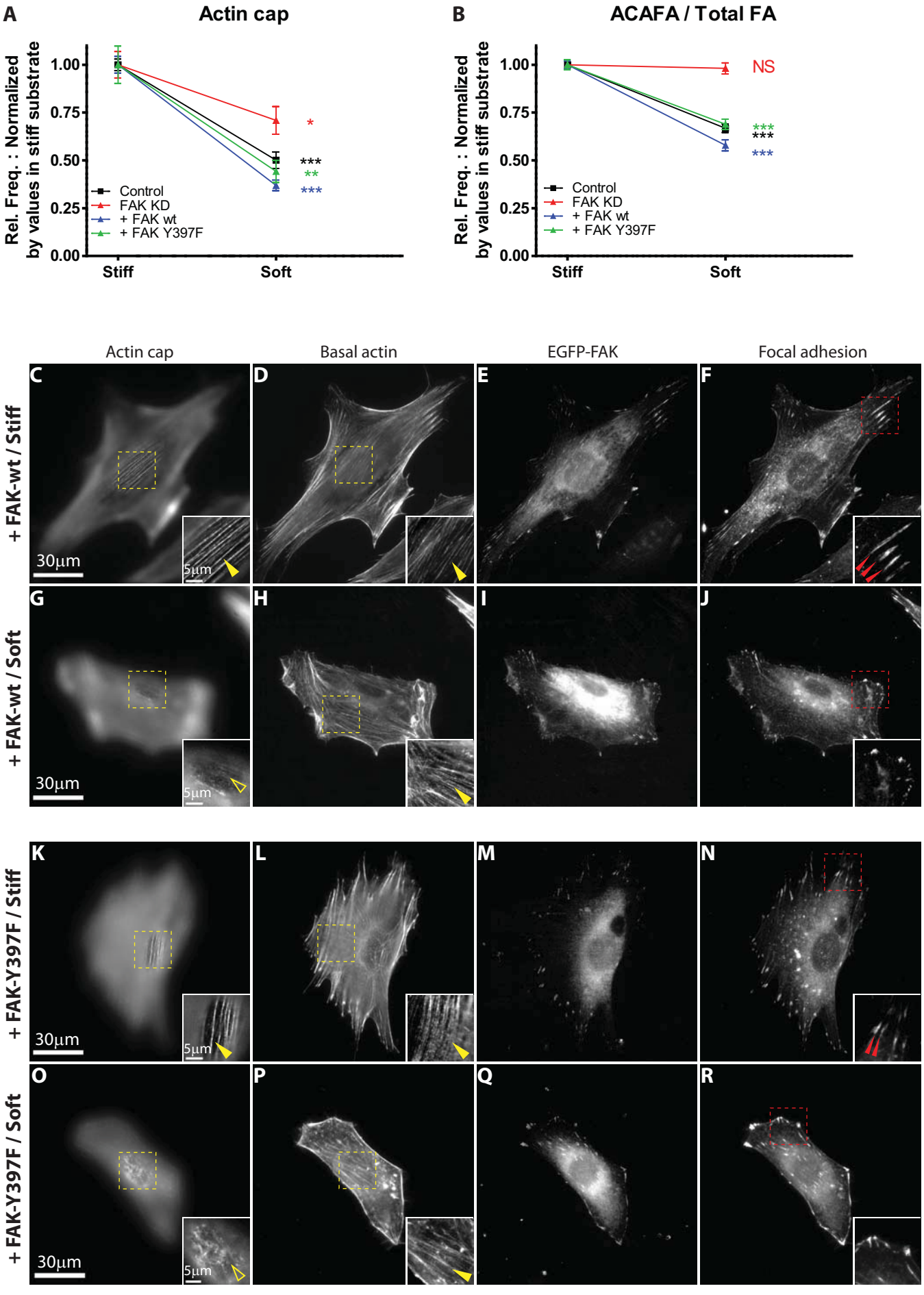
A
Actin cap
Rel. Freq. : Normalized by values in stiff substrate
1.00
0.75
0.50
0.25
0.00
Control
FAK KD
+ FAK wt
+ FAK Y397F
*
***
**
***
Stiff
Soft
B
ACAFA / Total FA
NS
***
***
***
Actin cap
Basal actin
EGFP-FAK
Focal adhesion
+ FAK-wt / Stiff
+ FAK-wt / Soft
+ FAK-Y397F / Stiff
+ FAK-Y397F / Soft
C
D
E
F
G
H
I
J
K
L
M
N
O
P
Q
R
30µm
5µm

Figure S8

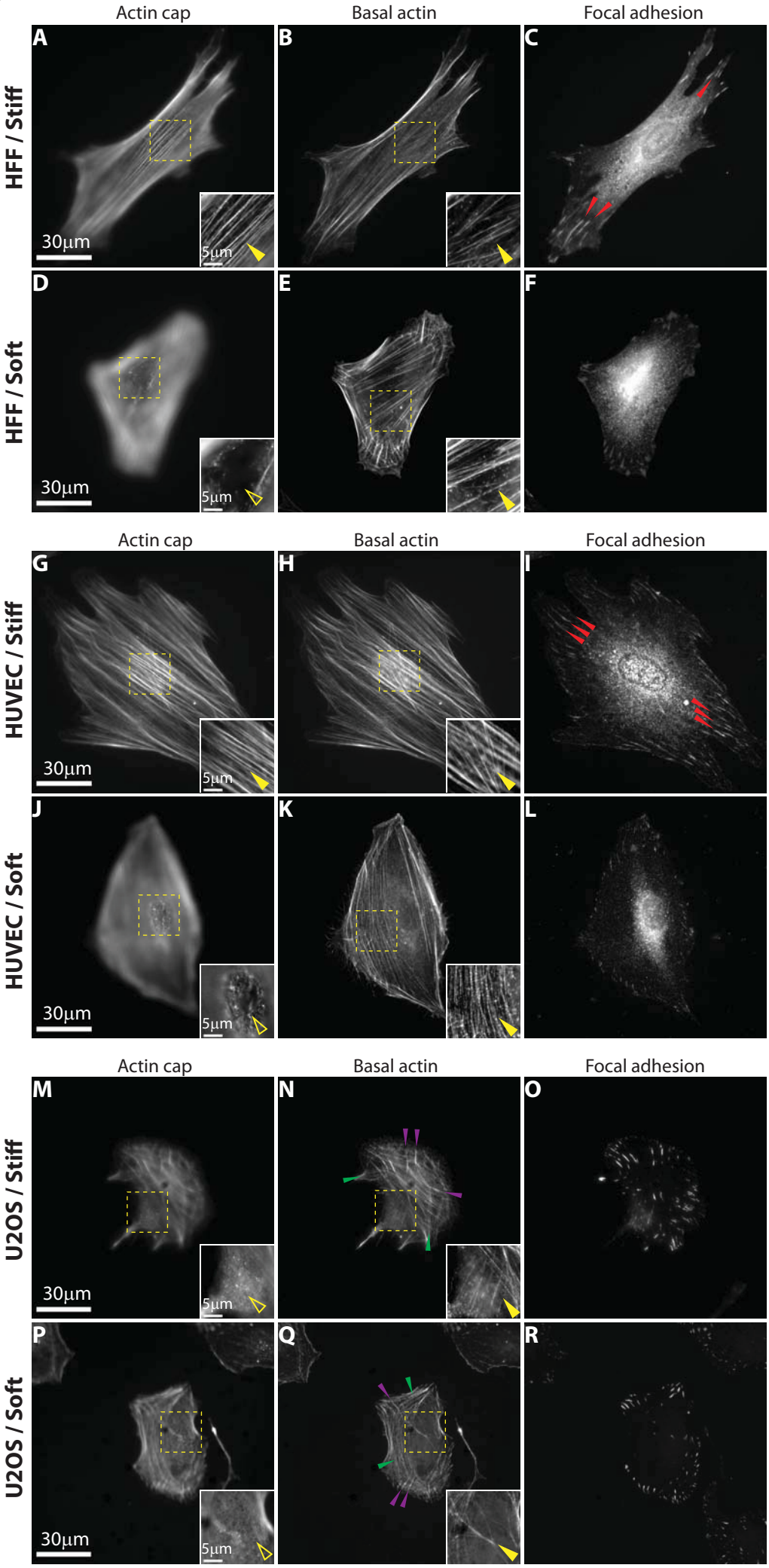
Actin cap
Basal actin
Focal adhesion
HFF / Stiff
HFF / Soft
HUVEC / Stiff
HUVEC / Soft
U2OS / Stiff
U2OS / Soft
A
B
C
D
E
F
G
H
I
J
K
L
M
N
O
P
Q
R
30μm
5μm

Figure S9

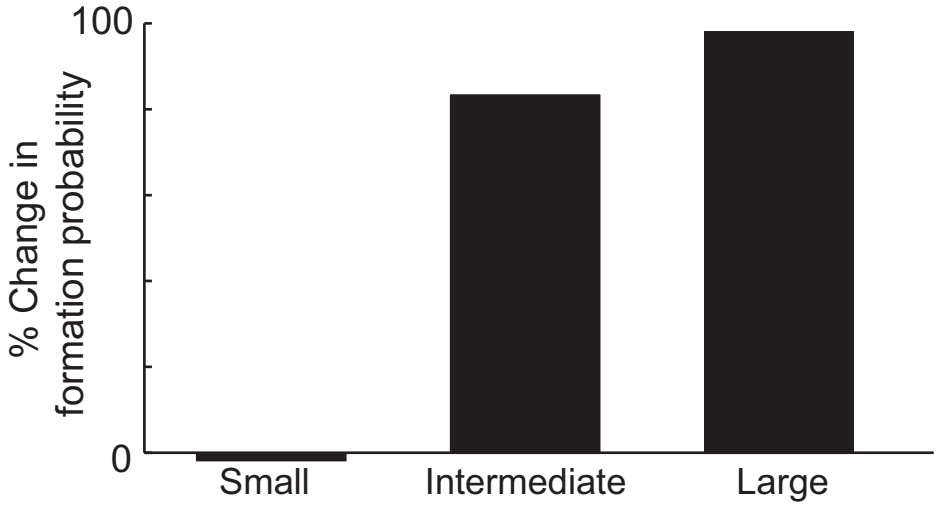
100
0
% Change in formation probability
Small
Intermediate
Large

Figure S10

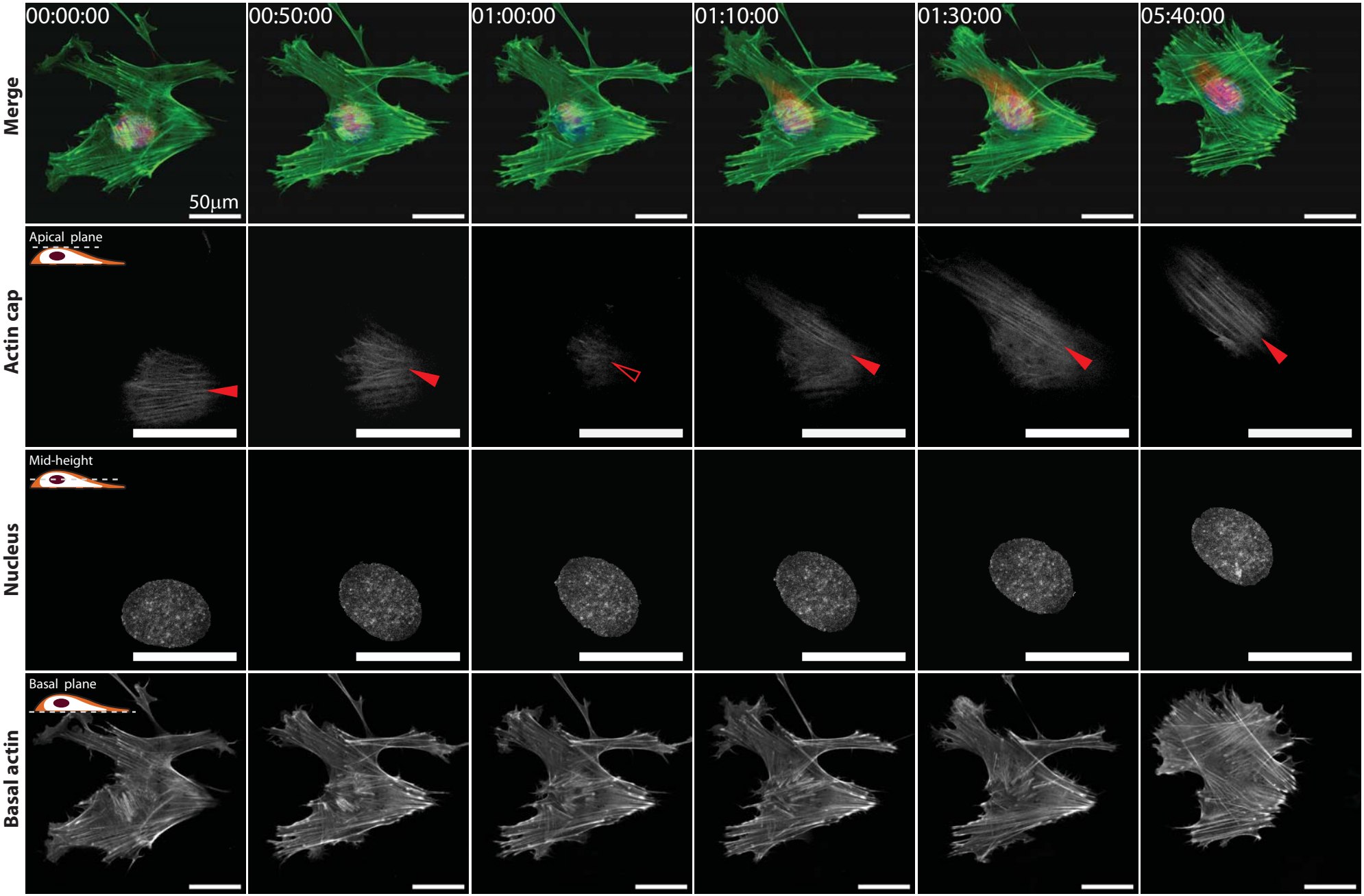
00:00:00
00:50:00
01:00:00
01:10:00
01:30:00
05:40:00
Merge
50μm
Actin cap
Apical plane
Nucleus
Mid-height
Basal actin
Basal plane

Legends to supplementary figures S1 to S10

Figure S1. Role of α-actinin and myosin II in the formation of actin cap and associated focal adhesions. A-I. Organization of actin cap fibers (A, D, G), basal actin fibers (B, E, H), and focal adhesions (C, F, I) in control cells (A-C), α-actinin-depleted cells (D-F), α-actinin-depleted cells treated with MLCK inhibitor ML-7 (G-I). ***Insets*** show details of the organization of stress fibers either at the top of the nucleus (A, D, G) or at the basal surface of the cell (B, E, H). Full and open arrowheads point to organized and disorganized/absent F-actin structure, respectively.

Figure S2. **Differential response of actin cap associated focal adhesions to changes in substrate compliance**. **A-F**. Typical organization of actin cap associated focal adhesions (red) and conventional focal adhesions (yellow) for cells on stiff (A, C, E) and soft substrates (B, D, F) through staining of paxillin (A, B), FAK (C, D), and zyxin (E, F). ***Insets*** show details of (unlabeled) focal adhesions. **G and H**. Number per cell (G) and total area per cell (H) of actin cap associated focal adhesions (black bars) and conventional focal adhesions (white bars) stained with vinculin, paxillin, FAK, and zyxin on stiff and soft substrate. **I-L**. Length (I), breadth (J), and shape factor (K), and speed of the centroids (L) of actin cap associated focal adhesions (black bars) and conventional focal adhesions (white bars) on stiff and soft substrates. In panel G and H, 30 cells were analyzed for each condition; In panel I-K, at least 300 focal adhesions per condition were examined for each condition; In panel L, 6 to 20 focal adhesions were monitored by time-lapse confocal microscopy; ***: $P < 0.001$; **: $P< 0.01$; *: $P < 0.05$; NS: $P > 0.05$.

Figure S3. **Changes in F-actin, focal adhesion structure, and cell size in response to changes in substrate compliance. A-F** F-actin (green), vinculin marked focal adhesion (red), and nucleus (DAPI, blue) were visualized by z-stacking images taken by confocal microscope in a low magnification (20x, A-C)

and high magnification (60x, D-F). Maximum intensity projection image in XY plane and 3D reconstructed XZ and YZ images of a selected cell are shown together (D-F). As substrate compliance increases, well organized actin cap fibers and actin cap associated focal adhesions in stiff substrate (A, D) disassembled earlier than basal stress fibers and conventional focal adhesions (B, E) and in the extremely soft substrate, most of organized F-actin structure was disrupted and no focal adhesions were detected (C, F). **G**. Average mean size of cells on subsrate of different compliance. ***: $P < 0.001$; **: $P < 0.01$. At least 50 cells were measured per condition.

Figure S4. **Changes in the ratio of pFAK contents in response to substrate compliance**. **A and B**. Average light intensity of pFAK[Y397] as a function of the average light intensity of FAK for individual actin cap associated focal adhesions (closed circles) and individual conventional focal adhesions (open circles) in cells on stiff (A) and soft (B) substrates. Red and blue lines show the linear fits of both types of focal adhesions and corresponding bar graphs show the averaged pFAK intensity normalized by FAK intensity per cell. Cells were fixed and stained at the same time using identical primary and secondary antibodies and visualized with identical camera settings. In panel A and B, 20 to 30 cells were analyzed per substrate and each cell had ~10 actin cap associated focal adhesions and ~40 conventional focal adhesions. ***: $P < 0.001$; NS: $P > 0.05$.

Figure S5. Differential content of vinculin in actin cap associated focal adhesions and conventional focal adhesions. Fluorescence intensity in vinculin staining for individual actin cap associated focal adhesions and conventional focal adhesions in cells. Cells grown onto collagen-coated stiff substrate were fixed, stained, and visualized with identical camera settings. Fluorescence intensity per area of focal adhesion (Vinculin intensity) of two types of focal adhesions was averaged per cell. 39 cells were tested and each cell had ~10 actin cap associated focal adhesions and ~40 conventional focal adhesions. Values rescaled from 0 to 1. ***: $P < 0.001$.

Figure S6. **Depletion of FAK, paxillin, talin, zyxin, and α-actinin in MEFs**. Western blots showing the depletion of FAK, paxillin, talin, zyxin, and α-actinin. Only cells depleted of >85% of the targeted protein were used for the studies in this paper. Western blots for: **A.** FAK and β-tubulin in control cells + mock vector, cells + luciferase vector, cells + sh-507, and cells + sh-661. **B.** Paxillin and β-tubulin in control cells + mock vector, cells + luciferase vector, cells + sh-1325, and cells + sh-1770. **C.** Talin 1,2 and β-tubulin in control cells + mock vector, cells + luciferase vector, cells + sh-1372, and cells + sh-6725. **D.** Zyxin and β-tubulin in control cells + mock vector, cells + luciferase vector, cells + sh-1004, and cells + sh-1484. **E.** α-Actinin 1,4 and β-tubulin in control cells + mock vector, cells + luciferase vector, cells + sh-1164, and cells + sh-1299. See more details in the Methods section.

Figure S7. Recovery of mechanosensing by reintroducing FAK in FAK-depleted cells. A and B. Relative changes in the fractions of cells showing an organized perinuclear actin cap (A) and number of actin cap associated focal adhesions divided by the total number of focal adhesions (B) normalized by corresponding values on stiff substrates (i.e. on stiff, the value is always 1), for control WT cells, cells depleted of FAK (FAK KD), and FAK-depleted cells where either EGFP-FAK (+ FAK WT) or FAK Y397F with an autophosphorylation site mutation (+ FAK Y397F) were re-introduced. The introduction of either wt FAK or Y397F FAK rescued the mechanosensory response of FAK-depleted cells to the level of control WT cells. **C-R.** Status of actin cap fibers (C, G, K, O), basal stress fibers (D, H, L, P), EGFP-FAK (E, I, M, Q), and focal adhesions (F, J, N, R) in EGFP-FAK-wt transfected FAK depleted cells on stiff substrates (C-F) and soft substrates (G-J) or in EGFP-FAK-Y397F transfected FAK depleted cells on stiff (K-N) and soft (O-R) substrates. ***Insets*** show details of actin cap and basal stress fibers, and focal adhesions. Full and open yellow arrowheads indicate well organized (C, D, H, K, L, P) or disrupted/absent (G, O) stress fibers, respectively. Red arrowheads indicate

actin cap associated focal adhesions (F and N) and conventional focal adhesions were unlabelled (F, J, N, R).

Figure S8. **Actin cap and actin cap associated focal adhesions also mediate mechanosensing in human cells.** Status of actin cap fibers (A, D, G, J, M, P), basal stress fibers (B, E, H, K, N, Q), actin cap associated focal adhesions (red arrowheads, C, I), and conventional focal adhesions (unlabeled, C, F, I, L, O, and R) in primary human foreskin fibroblasts (HFF), primary human umbilical vein endothelial cells (HUVEC), and human osteosarcoma cells (U2OS) on stiff (A-C, G-I, M-O) and soft (D-F, J-L, P-R) substrates. Dorsal stress fibers and transvers arcs in U2OS cells are indicated by purple and green arrowheads, respectively (N, Q). ***Insets*** show details of actin cap and basal stress fibers. Full and open arrowheads point to organized and disorganized/absent actin stress fibers, respectively.

Figure S9. Computational model of why larger focal adhesions are more sensitive to substrate compliance. Using a mechanical model for stress fiber formation [28], we predict that the probability of forming large focal adhesions decreases drastically as substrate compliance increases. Conversely, small focal adhesions do not respond to changes in the substrate compliance as much as larger focal adhesions. While the probability of forming large and intermediate-sized focal adhesions decreases by 83.4% and 98.2%, respectively, over the experimental range, the probability of forming small adhesions increases by only 1.8%. Percent changes in the plot were normalized by the probability on stiff substrates. In accordance with immunostaining results (Fig. S3, C and D), no measurable focal adhesions are formed on the extremely soft substrate. See more details in the Method section.

Figure S10. The conversion of actin cap fibers into basal actin fibers. Actin fibers in the apical plane (red) and basal plane (green), and nucleus in the mid-height (purple) in merged images (first row). Actin cap fibers in the apical region

of the cell were re-colored red to distinguish from basal actin fibers colored green. A cell transfected with GFP-lifeact and stained with DRAQ5 to visualize actin stress fibers and nucleus, respectively, was simultaneously monitored by time-lapsed confocal microscopy. All scale bars are 50 μm. Distance from the top to the bottom of the cell is 4.8 μm; the z-step was 0.8 μm during the live cell imaging. Images were captured every 10 min for 6 h. Actin cap fibers were gradually disrupted as the nucleus moved away from its initial position (~1h). When the nucleus was repositioned underneath nearby basal actin fibers, new actin cap fibers became progressively detectable above the nucleus (1h 10min~). Finally, new actin cap fibers tightly covered the whole area of the nucleus (5h 40min). Presence and disruption (or absence) of actin cap fibers are denoted by full and open red arrowheads, respectively. See also supplementary movie 3.

Legends to supplementary movie 1 to 3

Supplementary Movie 1. 3D reconstruction of actin organization. A mouse embryonic fibroblast cultured on the collagen coated glass substrate (denoted by “stiff” in the paper) was fixed and stained with phalloidin to visualize actin stress fibers. 3D reconstruction and cross-sectioning through the z axis were performed. To avoid visual distortion, DAPI stained nucleus was excluded. The width, length, and depth of the imaged cell are 45.8, 93.2, and, 2.2 μm, respectively and z-step is 0.22 μm. Note that at the center of the cell where nucleus is located, actin stress fibers organize a dorm shaped structure with actin cap (see XZ and YZ planes). By gradually moving the XY cross sections basal stress fibers which have diverse directions are shown on the whole basal plane of the cell, but actin cap fibers aligned to the cell body stretched direction were detected at the top plane. This movie shows perinuclear actin cap is distinct from basal stress fibers which are lying flat on the basal plane of the cell.

Supplementary Movie 2. Live-cell confocal imaging of actin cap associated focal adhesions and conventional focal adhesions. A cell was transfected with RUBY-lifeact to image F-actin and EGFP-paxillin to image both actin filament dynamics and focal adhesions. Actin cap associated focal adhesions were identified by following stress fibers from the top of the nucleus down to terminating focal adhesions at the basal surface of the cell by lowering the plane of focus. White arrow at the start of the movie points to one of the actin cap fibers followed from the top of the nucleus down a terminating actin cap associated focal adhesion. During the movie, that actin cap associated focal adhesion is indicated by a red arrow; a conventional focal adhesion (terminating a conventional stress fiber lying entirely in the basal layer of the cell) is indicated by a yellow arrow. This movie shows that actin cap fibers can turn into conventional stress fibers as they slide on the nuclear surface and eventually fall at the bottom of the cell to become conventional stress fibers.

Accordingly, actin cap associated focal adhesions become conventional focal adhesions.

Supplementary Movie 3. Live-cell confocal imaging showing the conversion of actin cap fibers into basal stress fibers due to nuclear movements. Imaging a live mouse embryonic fibroblast transfected with green-lifeact and stained with DRAQ5 clearly visualizes how actin cap fibers become conventional fibers due to the interaction with the nucleus. Here, actin cap fibers in the apical region of the cell were re-colored red, nucleus stained by DRAQ5 in the mid-height was colored purple, and basal stress fibers were colored green in the basal plane. While actin cap fibers push the nucleus, nucleus is moving away from the actin cap fibers, which subsequently become the basal stress fibers due to the loss of the underlying nucleus. Note that the long axis of the nucleus coincide with the orientation of actin cap fibers and nucleus rotates while escaping from the actin cap fibers (see also Fig. S10).